Heart rate variability covaries with amygdala functional connectivity during voluntary emotion regulation

NeuroImage 274 (2023) 120136

Contents lists available at ScienceDirect

NeuroImage

journal homepage: www.elsevier.com/locate/neuroimage

Heart rate variability covaries with amygdala functional connectivity during voluntary emotion regulation

Emma Tupitsa[a], Ifeoma Egbuniwe[a], William K. Lloyd[a,b], Marta Puertollano[a], Birthe Macdonald[a,c], Karin Joanknecht[a], Michiko Sakaki[d,e], Carien M. van Reekum[a,*]

[a] Centre for Integrative Neuroscience and Neurodynamics, School of Psychology and Clinical Language Sciences, University of Reading, Earley Gate, Whiteknights Campus, Reading RG6 6AL, UK
[b] School of Health Sciences, University of Manchester, Manchester, UK
[c] URPP Dynamics of Healthy Ageing, University of Zurich, Zurich, Switzerland
[d] Hector Research Institute of Education Sciences and Psychology, University of Tübingen, Tübingen, Germany
[e] Research Institute, Kochi University of Technology, Kochi, Japan

ARTICLE INFO

Keywords:
Heart rate variability
Neurovisceral integration model
Amygdala
Medial prefrontal cortex
Functional connectivity

ABSTRACT

The Neurovisceral Integration Model posits that shared neural networks support the effective regulation of emotions and heart rate, with heart rate variability (HRV) serving as an objective, peripheral index of prefrontal inhibitory control. Prior neuroimaging studies have predominantly examined both HRV and associated neural functional connectivity at rest, as opposed to contexts that require active emotion regulation. The present study sought to extend upon previous resting-state functional connectivity findings, examining task-related HRV and corresponding amygdala functional connectivity during a cognitive reappraisal task. Seventy adults (52 older and 18 younger adults, 18–84 years, 51% male) received instructions to cognitively reappraise negative affective images during functional MRI scanning. HRV measures were derived from a finger pulse signal throughout the scan. During the task, younger adults exhibited a significant inverse association between HRV and amygdala-medial prefrontal cortex (mPFC) functional connectivity, in which higher task-related HRV was correlated with weaker amygdala-mPFC coupling, whereas older adults displayed a slight positive, albeit non-significant correlation. Furthermore, voxelwise whole-brain functional connectivity analyses showed that higher task-based HRV was linked to weaker right amygdala-posterior cingulate cortex connectivity across older and younger adults, and in older adults, higher task-related HRV correlated positively with stronger right amygdala-right ventrolateral prefrontal cortex connectivity. Collectively, these findings highlight the importance of assessing HRV and neural functional connectivity during active regulatory contexts to further identify neural concomitants of HRV and adaptive emotion regulation.

1. Introduction

The ability to flexibly respond to ongoing and complex changes in our environment, in both a timely and contextually appropriate manner, is crucial for successful adaptation to environmental challenges and emotion regulation (Aldao et al., 2015; Thompson, 1994). Responses to such situational demands generates a cascade of changes at both subjective (e.g., emotional states, expressions) and physiological (e.g., elevations or reductions to heart rate, sweating, heightened neural responding) levels. Heart Rate Variability (HRV), physiologically defined as the variation in time intervals between consecutive heart beats, has increasingly been employed as an objective, peripheral measure to capture individual differences in adaptive autonomic responding and self-regulatory capacity, including emotion regulation (Appelhans and Luecken, 2006).

Resting HRV reflects the predominance of the parasympathetic branch of the autonomic nervous system (ANS). Both the sympathetic and parasympathetic branches directly innervate the heart via the stellate ganglia and vagus nerve respectively (Berntson et al., 1997). Dynamic interplay between both branches produces complex variations in the heart rate period that is captured by HRV, but it is the fast, modulatory impact of the parasympathetic nervous system (via the vagus nerve) that reportedly exhibits the strongest influence on the heart's pacemaker (i.e., sinoatrial node) and subsequent variation in heart rate, particularly at rest (Berntson et al., 1997). Greater variation in the time intervals between successive heart beats (Root Mean Square of Successive Differences, RMSSD) and dominance of high frequency (HF) heart rate oscillations (HF-HRV) are HRV parameters that capture the predominance of the parasympathetic branch of the ANS (Shaffer and Gins-

* Corresponding author.
E-mail address: c.vanreekum@reading.ac.uk (C.M. van Reekum).

https://doi.org/10.1016/j.neuroimage.2023.120136.
Received 16 December 2022; Received in revised form 19 March 2023; Accepted 25 April 2023
Available online 26 April 2023.

berg, 2017). Typically, higher levels of HRV at rest indicate a more adaptive and responsive cardiovascular system, supporting fast and flexible alterations in physiological responses to effectively manage stressors, as well as maintaining homoeostasis (Shaffer and Ginsberg, 2017; but see Kogan et al. (2013) for discussion on the quadratic nature of HRV).

Several models discuss the role of HRV in adaptive psychophysiological responding (Grossman and Taylor, 2007; Laborde et al., 2018; Porges, 2007, 2011; Smith et al., 2017; Thayer and Lane, 2000, 2009). In particular, the Neurovisceral Integration Model (NIM; Smith et al. 2017; Thayer and Lane 2000, 2009) outlines a complex and reciprocal network of neural regions that overlap to support autonomic, cognitive and affective regulatory processes. At the heart of the NIM is the 'central autonomic network' (CAN; Benarroch, 1993), which encompasses higher cortical structures (e.g. ventromedial prefrontal cortex, anterior cingulate cortex), subcortical limbic regions (e.g. central nucleus of the amygdala, hypothalamus) and brainstem structures (e.g. periaqueductal gray, parabrachial nucleus), forming a vital, coordinated network that facilitates autonomic function and regulation (Benarroch, 1993; Thayer et al., 2009a). The NIM posits that the prefrontal cortex exerts tonic inhibitory control over subcortical structures, and by extension the vagus nerve. As such, resting HRV is proposed to serve as an index of the effective functioning of inhibitory cortical-subcortical connectivity and Central Nervous System-Autonomic Nervous System integration, in turn promoting adaptive self-regulation (Thayer and Lane, 2000, 2009; Thayer et al., 2009a).

A growing body of neuroimaging research lends support for the NIM and the link between resting HRV and emotion regulation-related brain function (Mather and Thayer, 2018; Sakaki et al., 2016; Schumann et al., 2021a; Steinfurth et al., 2018). A prior meta-analysis highlighted significant and consistent associations between HRV and cerebral blood flow in the mPFC (including rostral and subgenual anterior cingulate regions) and the amygdala across several studies (Thayer et al., 2012). Importantly, despite reported reductions in resting HRV with age (Agelink et al., 2001; Russoniello et al., 2013), both older and younger adults with relatively higher resting HRV exhibited stronger resting medial prefrontal cortex (mPFC)-amygdala functional connectivity (Nashiro et al., 2022; Sakaki et al., 2016). Higher HRV has also been linked to stronger resting amygdala-ventrolateral prefrontal cortex (vlPFC) connectivity in younger adults (Sakaki et al., 2016). Relatedly, a study conducted by Kumral et al. (2019) found that younger adults with higher resting HRV had stronger bilateral ventromedial prefrontal cortex (vmPFC) connectivity, with this vmPFC seed demonstrating further extended functional connectivity with several CAN regions. Increasing resting HRV via biofeedback interventions (e.g., slow breathing, Lehrer and Gevirtz, 2014) has been reported to elevate resting-state functional connectivity of the vmPFC to neural regions implicated in emotional processing and the NIM, including the amygdala, middle cingulate cortex, anterior insula, and lateral PFC (Schumann et al., 2021a). Interestingly, fewer studies have assessed HRV and associated neural activity during tasks that require emotional or self-regulatory processes. Higher resting HRV has previously been linked to increased vmPFC activation during an effortful self-control dietary task in younger adults (Maier and Hare, 2017). Moreover, while engaging in a voluntary emotion regulation task, younger adults with higher resting HRV more effectively recruited the dorsal medial prefrontal cortex to modulate amygdala responses via reappraisal (Steinfurth et al., 2018).

Collectively, prior research supports the notion that HRV serves as a measure of effective, inhibitory cortical-subcortical connectivity, with the PFC and amygdala showing consistent associations with HRV (Thayer et al., 2012). Relatedly, mPFC-amygdala interconnectivity has been reported to facilitate successful emotion regulation (Etkin et al., 2011). It has been suggested that medial regions of the prefrontal cortex support automatic or implicit forms of emotion regulation, whereas more lateral regions facilitate explicit emotion regulation (Braunstein et al., 2017; Phillips et al., 2008). Others propose that higher order, cognitive control regions (i.e., ventrolateral and dorsolateral prefrontal cortex) impart control messages to the amygdala via the vmPFC given stronger anatomical connections between the amygdala and mPFC (Buhle et al., 2014). Indeed, many of the brain areas identified in HRV neuroimaging studies overlap with regions that support implicit and explicit emotion regulation (Braunstein et al., 2017; Buhle et al., 2014; Morawetz et al., 2020; Wager et al., 2008).

Nonetheless, it is evident that previous research has largely assessed both HRV and neural functional connectivity predominantly at rest. Resting-state paradigms have recently received criticism in the literature, especially in relation to the utility, interpretability, and reliability of neural findings observed under resting-state contexts (Finn, 2021). Indeed, the state of 'rest' is increasingly being recognised as a 'task' in and of itself, with many unconstrained, internal state factors contributing to diverse cognitive states (Finn, 2021), including mind wandering and self-generated thoughts (Gorgolewski et al., 2014; Smallwood and Schooler, 2015), and drifts in sleep-wakefulness stages (Tagliazucchi and Laufs, 2014). Recent evidence has highlighted the potential advantage of demands imposed by task engagement, and how such demands may constrain underlying neural functional connectivity to reduce variance related to aforementioned internal state factors, in turn increasing sensitivity to detect individual differences of interest (Finn and Bandettini, 2021).

Relatedly, whilst resting HRV has most commonly been assessed in prior work, fewer studies have assessed HRV during tasks. A growing body of research has examined phasic changes in HRV, including phasic HRV changes in reactivity to, and recovery from, task-related stressors and events relative to baseline HRV levels (Butler et al., 2006; Denson et al., 2011; Park et al., 2014; Segerstrom and Nes, 2007; for a review see: Laborde et al. 2018). Empirical evidence supports the notion that phasic HRV increases are indicative of self-regulatory effort and emotion regulation success (Butler et al., 2006; Denson et al., 2011; Ingjaldsson et al., 2003; Park et al., 2014; Segerstrom and Nes, 2007). Crucially, resting levels of HRV has been found to modulate such phasic HRV increases (Park et al., 2014). For instance, women with higher resting HRV experienced greater phasic HRV increases during successful voluntary emotion regulation via reappraisal and emotional suppression in comparison to those with lower resting HRV (Butler et al., 2006). Phasic HRV increases have also been linked to greater activation in the subgenual anterior cingulate cortex, a region involved in emotion regulation (Lane et al., 2013). In a similar vein, strong positive associations have been reported between resting HRV and HRV assessed during stress (Wang et al., 2009) and a challenging working memory task (Heffner et al., 2022). Collectively, empirical evidence suggests that individuals with higher resting HRV are more likely to demonstrate phasic HRV increases when challenged by stimuli or events that require self-regulatory effort, reflecting more adaptive responding to task demands and successful emotion regulation.

Overall, since the NIM emphasises the role of inhibitory cortical-subcortical circuitry in supporting adaptive self-regulation, examining HRV and associated functional connectivity in contexts that require active engagement of emotion regulatory processes may help to further our understanding of heart-brain function in supporting emotion regulation. The current study sought to extend prior resting-state functional connectivity findings by assessing pulse-derived HRV and neural functional connectivity whilst participants actively engaged in a voluntary emotion regulation task in the scanner. As the pulse signal was acquired during the scan only, we aggregated HRV across the emotion regulatory context to derive task-related HRV. Based on empirical evidence from prior studies linking higher resting HRV to greater phasic HRV during emotion regulation (Butler et al., 2006; Denson et al., 2011), any phasic HRV increases during the reappraisal task in the current study would likely be captured as elevated task-related HRV when aggregated across the entire duration of the task. Also, considering that HRV is positively correlated within individuals across contexts (Heffner et al., 2022; Wang et al., 2009), the relative rank order of task-related HRV metrics across individuals during a reappraisal task should be similar to that observed dur-

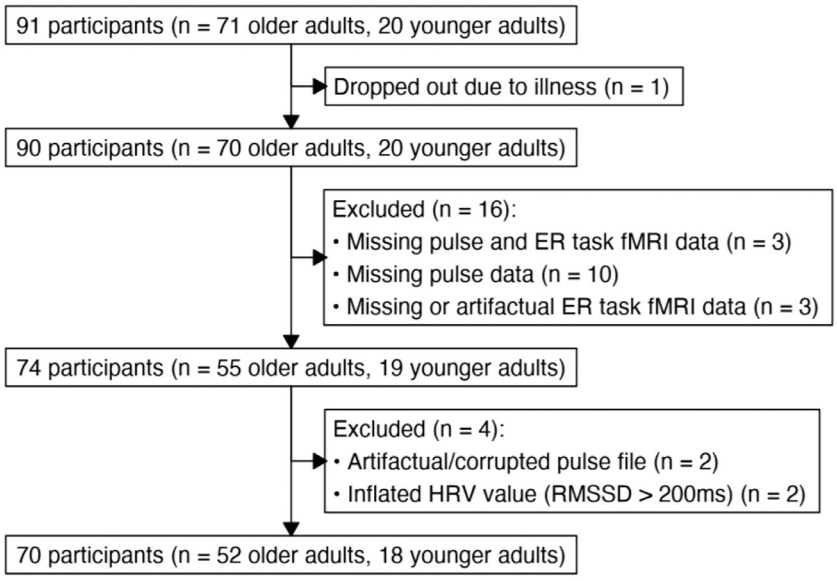

Fig. 1. Participant selection and exclusion process. Participants were selected from a larger pool of subjects recruited as part of a wider ageing study.

ing rest (i.e., individuals with lower resting HRV will likely exhibit lower task-based HRV compared to those with higher resting, and thus higher task-based, HRV). Extrapolating from prior resting-state HRV studies, considering the shared role of the mPFC in HRV control and emotion regulation, we hypothesised that task-related HRV would be positively associated with stronger functional connectivity between the amygdala and the mPFC. The mPFC seed region used in the present study was previously adopted as a region of interest in Sakaki et al. (2016) and demonstrated robust associations with resting HRV. Specifically, we predicted that individuals with higher task-related HRV would exhibit stronger positive amygdala-mPFC functional connectivity during a cognitive reappraisal task. Given that pulse recordings were obtained concurrently in the scanning session with the reappraisal task, our primary focus was to examine the relationship between HRV and amygdala connectivity in an emotion regulation context, adopting a functional connectivity analysis similar to that performed on resting-state data (e.g., calculating functional connectivity during the reappraisal task). However, for conceptual replication and comparative purposes, we further assessed task-related HRV and associated resting-state functional connectivity acquired during an initial scanning session that took place 1-2 weeks prior to the session where the task-related HRV measures were obtained. For transparency, further details and results are presented in the Supplementary Material.

2. Materials and method

2.1. Participants

Participants in the current study were derived from a larger sample of 91 subjects (71 older adults, 20 younger adults) previously recruited as part of an ageing research project (Lloyd et al., 2021; https://openneuro.org/datasets/ds002620).[1] Participants were recruited via the University of Reading's Older Adult Research Panel and through local poster and newspaper advertisements in Reading. Participants received financial compensation (£7.50 per hour) for their participation. From the overall sample, 74 participants (55 older adults, 19 younger adults) had both emotion regulation task-based functional magnetic resonance imaging (fMRI) and pulse data. Fig. 1 illustrates the participant selection and exclusion process. Following exclusion, 70 participants (52 older and 18 younger adults, aged 18–84 years, *M* age = 58.27 years, SD = 20.33; 51% male) were considered for analyses (see Table 1 for details per age group).

All participants were right-handed and reported no history of neurological disorder. Medical history and medication details were obtained for the older adults only. Of the older adults included in the study (N = 52), 15 disclosed taking regular medication for blood pressure and/or cardiovascular health: statins (N = 8), angiotensin-converting enzyme inhibitors (N = 2), angiotensin receptor blockers (N = 2), calcium channel blockers (N = 2) and beta-blockers (N = 1). The remaining 37 participants did not report use of medication related to cardiovascular health. Furthermore, 21 participants reported having experienced a cardiovascular health condition: high blood pressure (N = 12), high cholesterol (N = 6) and mini-stroke (N = 3). Given that we did not observe significant differences in task-related HRV between those taking cardiovascular medication ($t(50) = -0.46$, $p = .647$, $d = -0.14$) and those who disclosed a history of cardiovascular disease ($t(50) = -0.70$, $p = .485$, $d = -.20$), with participants who did not report use of cardiovascular medication and/or a history of cardiovascular disease, we opted to retain these older adults in the analyses.

The research study from which the current sample was derived was carried out in accordance with the Declaration of Helsinki (1991, p.1194). The study's procedures were given a favourable ethical opinion of conduct by the University of Reading's Research Ethics Committee and NHS Research Ethics Service. Participants provided written informed consent prior to their participation.

2.2. Materials and procedure

2.2.1. Cognitive reappraisal task

Participants engaged in a voluntary emotion regulation task during the scan, which followed an established cognitive reappraisal paradigm employed by previous research (e.g., van Reekum et al. 2007). Cognitive reappraisal is an antecedent-focused strategy that requires an individual to reinterpret or alter the meaning of an emotional event (Gross and John, 2003). A detailed description of the reappraisal task and stimuli can be found in Lloyd et al. (2021).

The cognitive reappraisal task comprised 96 trials in total, in which 72 negative and 24 neutral pictures obtained from the International Af-

[1] The original research project sought to examine associations between neural function, cognitive function, and emotion regulation within an older adult population. A smaller sample of younger adults matched for gender and education level were recruited as an additional control for age in the original study.

Table 1
Participant characteristics (age, sex, HRV-related metrics, amygdala-mPFC connectivity and self-reported negative emotional intensity ratings for each task condition) across the whole sample and each age group. Data is provided in means and standard deviations (in parenthesis).

	Whole Sample (18–84 years) (N = 70)	Older Adults (55–84 years) (N = 52)	Younger Adults (18–35 years) (N = 18)
Demographics			
Age (years)	58.27 (20.33)	69.34 (8.08)	26.28 (4.75)
Sex (%)	49% F/51% M	44% F/56% M	61% F/39% M
lnRMSSD (ms)	4.01 (0.54)	3.92 (0.55)	4.29 (0.44)
Heart Rate (BPM)	67.60 (17.64)	64.61 (9.78)	76.24 (29.48)
RR Interval (ms)	937.73 (156.19)	959.80 (141.43)	873.97 (182.24)
fMRI Variables			
Right Amygdala-mPFC Connectivity (PE)	0.03 (0.13)	0.02 (0.11)	0.05 (0.16)
Left Amygdala-mPFC Connectivity (PE)	0.03 (0.11)	0.02 (0.10)	0.05 (0.11)
Emotion Intensity Ratings			
Enhance	2.78 (0.39)	2.75 (0.41)	2.88 (0.31)
Suppress	2.62 (0.35)	2.58 (0.37)	2.73 (0.28)
Maintain (Negative)	2.60 (0.33)	2.56 (0.33)	2.73 (0.30)
Maintain (Neutral)	1.26 (0.41)	1.26 (0.30)	1.28 (0.63)

lnRMSSD, natural log transformed root mean square of successive differences; ms, milliseconds; BPM, beats per minute; PE, mean parameter estimate (beta value).

fective Picture System (IAPS; Lang et al. 2008) were presented. On a given trial, participants were instructed to either "suppress" (decrease), "enhance" (increase), or "maintain" their emotional response and attend to the image presented (neutral images were always paired with the "maintain" instruction).[2] The "suppress" instruction in this task involved imagining an outcome less negative than the participant's original thoughts and/or feelings towards the image to reduce the intensity of any emotions experienced, as opposed to (expressive) suppression, a response-focused strategy that involves controlling emotion-expressive behaviors (Gross and John, 2003). The "enhance" instruction required imagining a worse or more negative outcome to increase the intensity of any emotions experienced. In the "maintain" condition, participants were instructed to simply attend to the image and sustain their emotional response. Following the presentation of the picture and engagement in the relevant auditory regulation instruction, a rating screen appeared for a fixed duration of three seconds, during which participants were asked to rate the intensity of their emotion in response to each image on a four-point scale (1 = neutral, 2 = somewhat negative, 3 = quite negative, 4 = very negative). Responses were recorded via a 4-button MR-compatible button box held in the participant's right hand and the button order was counterbalanced between subjects (1 = neutral, 4 = very negative or vice versa).

The scanning procedure was distributed across four identical runs, with 24 trials in each run. The duration of each run was approximately seven minutes, with rest breaks offered between runs, leading to an overall task duration of approximately 30 minutes.

2.3. Data reduction and analysis

2.3.1. HRV processing and analysis

A pulse signal was continuously recorded via an MRI-compatible pulse oximeter clip attached to the participant's left finger throughout the scanning session, including breaks (sampling rate = 50 Hz). The pulse oximeter was integrated with the Siemens Magnetom Trio MRI scanner, from which the raw pulse signal was subsequently extracted.

The raw pulse files underwent visual inspection for quality and usability prior to pre-processing and were formatted to read into LabChart software (version 8.1.11; AD Instruments, Oxford, UK). Initial manual edits within LabChart involved trimming the beginning and/or end of the file where flatlines and/or obvious calibration and motion-related noise were visually detected. Subsequently, LabChart files were converted and exported into LabChart text files to ensure compatibility with Kubios HRV Analysis software (version 2.2; Biosignal Analysis and Medical Imaging Group, University of Kuopio, Finland; Tarvainen et al. 2014). Further processing of the pulse signal and calculation of HRV measures were performed within Kubios. Taking into consideration variation in breaks between runs and tasks, alongside the quality of the pulse signal, participants had somewhat varying durations of pulse signal for analysis (range 17–76 min, M duration = 51 min). Occasionally, the automated peak detection feature either misplaced or missed the pulse peak, thus resulting in manual corrections to either place or (re)move markers to the peak of the pulse waveform. Following manual corrections, data were artifact-corrected using the "low" threshold setting (350 ms) across all participants to retain as many natural variations between heart beats as possible.

The Root Mean Square of Successive Differences (RMSSD), measured in milliseconds, and High-Frequency HRV (HF-HRV), defined using a frequency band of 0.15–0.40 Hz, measured in absolute power (ms^2, Fast Fourier Transform) were calculated within Kubios. Both measures were natural log transformed (ln) to correct for positive skew within RStudio (version 1.4.1106) using the 'log' command from the *base* package (v3.5.2). Despite variation in pulse duration, this did not demonstrate a significant correlation with either raw RMSSD ($r = -0.04$, $p = .747$) or natural log transformed RMSSD ($r = 0.03$, $p = .839$) values across participants ($N = 70$). Whilst RMSSD and HF-HRV metrics reflect parasympathetic vagal control, the RMSSD is a primary and robust measure of vagal tone (Kleiger et al., 2005), that is generally less susceptible to physiological noise, including respiratory influence (Hill et al., 2009). Also, given that both natural log transformed HRV measures exhibited a strong positive association in the current study ($r = 0.98$, $p < .001$), we proceeded with the (ln)RMSSD as our primary HRV metric for all analyses.

2.3.2. MRI procedure and image acquisition

Participants were invited to attend two different sessions within the Centre for Integrative Neuroscience and Neurodynamics (CINN) at the University of Reading. Structural and blood oxygenation level dependent (BOLD) functional imaging data were acquired using a 3T Siemens Magnetom Trio MRI scanner with a 12-channel head coil (Siemens Healthcare, Erlangen, Germany). The first session comprised an initial scanning protocol to obtain anatomical T1-weighted (T1w) struc-

[2] Participants received training and practice on the task prior to scanning to ensure that the regulatory strategies were used as intended (see Lloyd et al. (2021) for further details and the full instructions provided during the practice session). Furthermore, the words "suppress" and "enhance" were selected as opposed to "decrease" and "increase" to ensure that the auditory instruction for these conditions was distinctive.

tural scans, localisers and a resting-state scan (MRI acquisition details provided in Supplementary Material). Participants also engaged in several cognitive tasks outside of the scanner which are summarised elsewhere (Lloyd et al., 2021). The overall duration of the first session was approximately three hours (one hour scanning time). Participants were invited back for a second session which took place a few days (two weeks maximum) after the first session. For each participant, a 3D structural MRI was obtained via a T1-weighted sequence (Magnetization Prepared Rapid Acquisition Gradient Echo (MPRAGE)), repetition time (TR) = 2020 ms, echo time (TE) = 3.02 ms, inversion time (TI) = 900 ms, flip angle 9°, field of view (FOV) = 250 × 250 × 192 mm, resolution = 1 mm isotropic, acceleration factor = 2, averages = 2, acquisition time = 9 min, 7 s). Participants also performed two tasks whilst in the scanner: the cognitive reappraisal (emotion regulation) task and an emotional faces processing task. The emotion regulation fMRI data were obtained in four blocks of identical procedure, using an echo planar imaging (EPI) sequence (211 whole-brain volumes, 30 sagittal slices with *P>A* phase encoding, slice thickness = 3.0 mm, slice gap = 33%, TR = 2000 ms, TE = 30 ms, flip angle = 90°, FOV = 192 × 192 mm^2, resolution = 3 mm isotropic, acquisition time = 7 min 10 s per block). The participant's pulse was recorded throughout the scan. The overall duration of the second session was approximately two hours (one hour scanning time). Structural and emotion regulation fMRI task data are publicly available on OpenNeuro: https://openneuro.org/datasets/ds002620/versions/1.0.0.

2.3.3. MRI data pre-processing

Functional imaging data were pre-processed and analysed using FMRIB's Software Library (FSL, version 6.0; www.fmrib.ox.ac.uk/fsl; Jenkinson et al., 2012; Woolrich et al., 2009; Smith et al., 2004) and Analysis of Functional NeuroImages (AFNI, version 19.3.03; http://afni.nimh.nih.gov/afni ; Cox 1996). Initial pre-processing steps included: skull stripping (non-brain removal) using FSL's brain extraction tool (BET; Smith 2002), motion correction using MCFLIRT (Jenkinson et al., 2002), field-map correction to correct for potential magnetic field inhomogeneity distortions, spatial smoothing using a Gaussian kernel with a full-width half maximum (FWHM) of 5 mm and high-pass temporal filtering (Gaussian-weighted least squares straight line fitting with sigma = 50 s). Each subject's functional image was first co-registered to their high resolution T1-weighted image using linear boundary-based registration (BBR) and subsequently normalised to the Montreal Neurological Institute (MNI) 152 T1 2 mm template using a 12 degrees of freedom affine transformation via FMRIB's Linear Image Registration Tool (FLIRT).

Application of individual-level Independent Component Analysis (ICA) via FSL's Multivariate Exploratory Linear Optimized Decomposition into Independent Components (MELODIC; Beckmann and Smith 2004) separated the fMRI BOLD signal into a set of spatial maps (independent components) representing neural signal and/or noise. Independent components containing structured temporal noise, including scanner and hardware artifacts, physiological artifacts (respiratory and/or cardiac noise), and motion-related noise were identified via visual inspection and removed using the FSL command line tool '*fslregfilt*' for each emotion regulation task run (Griffanti et al., 2017). An average percentage of 72.07% components were removed across the four runs. This aligns with previous research that has typically identified >70% noise versus signal components in standard sequences at 3T (Griffanti et al., 2017).

Following ICA filtering, low bandpass filtering was applied to the fMRI data using AFNI's '*3dBandpass*' tool (Cox, 1996) to further remove confounding signals below 0.009 Hz and above 0.1 Hz. Prior to analysis, each subject's corresponding mean functional timeseries image was added back to the bandpass filtered data using '*fslmaths*' to ensure compatibility with FSL's FMRI Expert Analysis Tool (FEAT).

Average framewise displacement (FD) for each participant and task run was calculated using the realignment parameters generated after initial motion correction with FSL's MCFLIRT (Power et al., 2012) and after denoising (i.e., following ICA and low bandpass filtering) using FSL's '*fsl_motion_outliers*' to assess changes in motion. Participants or task runs were not initially excluded for exceeding a set mean FD threshold for several reasons. The exclusion of participants with higher motion can introduce selection bias, as greater movement in the scanner may be a marker that correlates with relevant (sociodemographic or clinical) variables of interest, which in turn risks data becoming missing not at random (Nebel et al., 2022). Furthermore, there is still not a universally accepted FD threshold in which volumes or functional data are considered as being contaminated by excess motion, especially as the sensitivity of this threshold is likely to vary as a function of subject and/or acquisition factors (Pham et al., 2023). Importantly, FD is calculated prior to further denoising techniques, which risks the premature removal of functional volumes, task runs, and/or subjects that may exhibit lower motion-related noise following further processing (Pham et al., 2023). Correspondingly, in the current study, average FD across all task runs was minimal following denoising (M = 0.02 mm, SD = 0.01 mm, range = 0.01–0.05 mm), and no single volume across subjects exceeded 0.2 mm, suggesting that motion had been reduced using the outlined techniques.

2.3.4. Functional connectivity analysis

Regions of interest (ROIs) were separate right and left amygdala seeds, and an area of the mPFC previously found to be correlated with HRV (Sakaki et al., 2016). Separate amygdala ROIs were selected given recent discrepancies in amygdala lateralisation with the mPFC as a function of HRV (Nashiro et al., 2022; Sakaki et al., 2016), and also observed lateralisation effects highlighted in previous research concerning emotion processing and regulation (Baas et al., 2004; Yang et al., 2020). Amygdala ROI masks were defined using the Harvard-Oxford Subcortical Probability atlas and thresholded at 80% probability (right amygdala: 114 voxels, 912 mm^3, centre of gravity: $x = 24$, $y = -3$, $z = -18$; left amygdala: 95 voxels, 760mm^3, centre of gravity: $x = -23$, $y = -5$, $z = -18$). The mPFC ROI contained voxels from the anterior cingulate cortex (ACC) and paracingulate gyrus thresholded at 25% probability (Harvard-Oxford atlas; 263 voxels, 2104mm^3, centre of gravity: $x = -1$, $y = 47$, $z = 8$). This mPFC area has previously been associated with memory positivity in older adults (Sakaki et al., 2013) but was more recently employed as a seed ROI in Sakaki et al. (2016), in which higher HRV was correlated with stronger amygdala coupling with this mPFC sub-region. Relatedly, both the ACC and mPFC have been shown to facilitate down-regulation of the amygdala (Etkin et al., 2011). All ROI masks (right and left amygdala, mPFC) were first transformed to each participant's native functional space using FSL's Apply FLIRT Transform '*ApplyXFM*' and binarised. Subsequently, the mean time series for each ROI was extracted from the four separate emotion regulation runs for each participant using '*fslmeants*'.

Separate first-level regression analyses were performed for each ROI using FEAT (Woolrich et al., 2001). Similar to a functional connectivity analysis typically performed on resting-state data, individual models included the mean time series extracted from the specific ROI and regressors of no interest, specifically: FSL's six standard head-motion parameters,[3] and average white matter and ventricular (CSF) signal. Average signal from white matter and CSF was extracted from masks generated via segmentation of each participant's high resolution T1w image using FMRIB's Automated Segmentation Tool (FAST; Zhang et al. 2001).

Inclusion of global signal regression (GSR) has received scrutiny in the literature and remains a controversial pre-processing technique (Murphy et al., 2009; Murphy and Fox, 2017; Uddin, 2017). Although

[3] Note that inclusion of the six rigid-body motion parameters compared to the extended 24 motion parameters (i.e., the six motion parameters, their derivatives, and the squares of these) in the single subject models made a negligible difference to the spatial maps and timecourses at both the lower-level and fixed effects FEAT level.

GSR is effective at removing global sources of noise, including physiological and motion artifacts (Li et al., 2019), the global signal is not wholly comprised of noise and its topography has been associated with important physiological, cognitive, and age differences (Bolt et al., 2022; Li et al., 2019; Nomi et al., 2022). Importantly, in task-based contexts, global signal is highly correlated with the task paradigm (Mayer et al., 2019). Given the controversy and lack of consensus surrounding GSR, we did not include GSR as a regressor in the model.

Furthermore, the task design was not included as a regressor in the model. It is recognised that not including the task design as a regressor in task-based functional connectivity analyses can result in spurious correlations and systematic inflation of functional connectivity estimates due to task-induced coactivations (Cole et al., 2019). Whilst techniques such as finite impulse response (FIR) task regression have been recommended to reduce the influence of spurious or inflated results corresponding to task-evoked activations (Cole et al., 2019), this approach may not be as effective when applied to relatively fast event-related fMRI designs. Crucially, the overarching aim of the present study was to examine HRV and associated neural functional connectivity in a voluntary emotion regulation context. Since the visual presentation of the images and emotion regulatory processes were designed to be perfectly confounded in the reappraisal task, and HRV is also closely related to, and considered a metric of, regulatory ability, if task activation events that mainly reflect variation in emotion regulatory processes were to be regressed from the data, any brain coactivation with HRV would then be derived from residualised data, without the emotion regulatory context. Moreover, not regressing the task design has been reported to increase the reliability of functional connectivity measures (Cho et al., 2021). For these reasons, task design was not included as a regressor in the models.

Prior to group-level analyses, a second-level fixed effects analysis using FSL's FEAT was applied to the emotion regulation task-based fMRI data to collapse the ROI connectivity maps across the four task runs.[4] This generated mean positive and negative functional connectivity maps for input to higher-level analyses.

2.3.5. Amygdala-mPFC functional connectivity analyses

Beta values (mean positive parameter estimates) from right and left amygdala connectivity maps were extracted using FSL's Featquery, with the mPFC seed as the reference mask. The corresponding beta values served as an index of amygdala-mPFC connectivity strength.

Multiple regression analyses were employed to examine associations between task-related HRV and amygdala-mPFC functional connectivity strength in the whole sample. Separate multiple regression models were tested with (i) right amygdala-mPFC connectivity and (ii) left amygdala-mPFC connectivity values as dependent variables. A segregation in age (years) was observed between the older and younger adults, leading to a natural formation of two separate age groups (see Fig. S2 in the Supplementary Material). We therefore entered age as a categorical predictor in the regression models. The following predictors were entered into the regression model: age group (1 = older adults, 0 = younger adults), (ln)RMSSD (centered), and a HRV x age interaction term.[5] In each model, age group and HRV were entered first (step 1), followed by the HRV x age interaction predictor (step 2). Standardised beta coefficients are reported for all predictors in the Results.

2.3.6. Whole-Brain functional connectivity analyses

Given the heterogeneous neurological profiles often observed in ageing brains (Chen et al., 2016), and the larger sample of older adults in the current study, we performed whole-brain functional connectivity analyses for all ROIs across the whole sample, including age as a blocking factor in the analyses, and further performed separate whole-brain analyses restricted to the older adult sample only. This allowed us to be more inclusive in our search for functionally-relevant regions associated with HRV that may have been excluded or otherwise missed using a ROI approach. Furthermore, the decision to run separate whole-brain connectivity analyses restricted to adults in the older age group was primarily driven by the unequal number of older relative to younger adults (and the comparative small sample size of the younger adult group), along with the strong effect of biological age on HRV (Agelink et al., 2001; Russoniello et al., 2013).

Whole-brain group analyses for each seed region were performed using FMRIB's Local Analysis of Mixed Effects (FLAME; Woolrich et al., 2004). The general linear model (GLM) included four explanatory variables: group mean and three predictors, HRV (lnRMSSD, centred), age (effect coded using +1 and −1 to define older and younger adult groups respectively) and a HRV by age interaction term (lnRMSSD centred x age group). Seven contrasts were entered into the model: group mean, HRV, age and the HRV by age interaction term (positive and negative contrasts for each EV). Clusters surviving a threshold of $Z > 3.1$ and correction for multiple comparisons with Gaussian random field theory (cluster significance: $p = 0.05$-corrected) were identified (Worsley, 2001). The locations of significant clusters that survived correction were labelled using the Harvard Oxford Cortical Structural and Subcortical atlases in MNI space within FSL. Mean beta values from significant clusters that emerged as a main effect of HRV were extracted for visualisation purposes.

3. Results

3.1. Descriptive statistics

Table 1 summarises general descriptives for the whole sample and for older and younger adult age groups separately. HRV significantly differed by age group, such that older adults demonstrated significantly reduced HRV as indexed by lower (ln)RMSSD values ($M = 3.92$, $SD = 0.55$), in comparison to younger adults ($M = 4.29$, $SD = 0.44$), $F(1,66) = 6.06$, $p = .016$, $\eta_p^2 = 0.08$. However, there was no significant difference in (ln)RMSSD values between females ($M = 4.07$, $SD = 0.52$) and males ($M = 3.96$, $SD = 0.57$) across the whole sample, $F(1,66) = 0.09$, $p = .764$, $\eta_p^2 = 0.00$, nor was there a significant interaction between age group and sex on (ln)RMSSD values, $F(1,66) = 0.15$, $p = .698$, $\eta_p^2 = 0.00$. Thus, no significant differences in HRV related to sex were observed in the present study (see Fig. S1 in the Supplementary Material). Additionally, there was a significant difference in the mean RR interval ($t(68) = 2.06$, $p = .044$, $d = 0.56$), but no significant difference in mean heart rate ($t(18) = -1.64$, $p = .117$, $d = -0.68$) between older and younger adults.

Moreover, in relation to self-reported ratings of negative emotional intensity, older and younger adults reported significantly greater negative emotional intensity after the enhance (increase) regulatory instruction ($M = 2.78$, $SD = 0.39$) relative to the maintain (attend) instruction ($M = 2.60$, $SD = 0.33$) in response to negative images ($t(69) = 4.76$, $p < .001$, $d = 0.57$). Counterintuitively, negative emotional intensity ratings were slightly higher for the suppress (decrease) regulatory instruction ($M = 2.62$, $SD = 0.35$) in comparison to the maintain instruction in response to negative pictures, but there was no significant difference in the ratings between these conditions ($t(69) = -0.52$, $p = .602$, $d = -0.06$). Overall, findings suggest that participants actively engaged in the reappraisal task and followed instructions to regulate, but reappraisal did not appear to significantly reduce negative affect beyond the control (maintain) condition.[6]

[4] Two participants were missing the final run of the emotion regulation task (run 4), so ROI connectivity maps were averaged across the three available task runs (runs 1-3) for these participants.

[5] To reduce the influence of multicollinearity that can occur between the original variables and the subsequent interaction that is comprised of those variables, the HRV x age interaction term was calculated by multiplying the centered (ln)RMSSD scores by the dummy coded age group.

[6] To target a more implicit metric of emotional reactivity, we examined differences in amygdala activation between the main regulatory conditions. Given

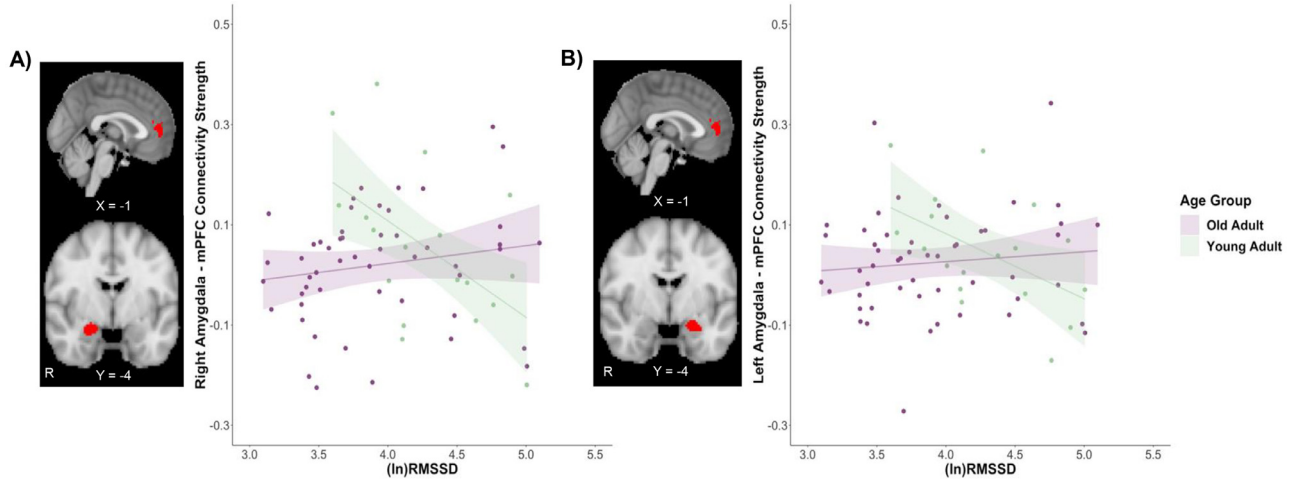

Fig. 2. HRV and amygdala-mPFC functional connectivity during the reappraisal task. (A) mPFC seed (top) and right amygdala seed (bottom). Significant HRV x age interaction for right amygdala-mPFC connectivity strength. In younger adults (light green), higher task-based HRV significantly predicted weaker connectivity between the right amygdala and mPFC, whereas a slight positive, albeit non-significant, association between task-related HRV and right amygdala-mPFC connectivity was observed in the older adults (purple). (B) mPFC seed (top) and left amygdala seed (bottom). Significant HRV x age interaction for left amygdala-mPFC connectivity strength. Similar to the right amygdala connectivity findings, in younger adults, greater task-related HRV significantly predicted weaker left amygdala-mPFC connectivity, whereas a non-significant, weak positive association between HRV and left amygdala-mPFC connectivity was observed in the older adults during the reappraisal task. *HRV, heart rate variability; mPFC, medial prefrontal cortex; (ln)RMSSD, natural* log *transformed root mean square of successive differences.*

3.2. HRV and amygdala-MPFC functional connectivity analysis

3.2.1. HRV and right amygdala-MPFC functional connectivity

Neither age ($\beta = -0.12$, $t = -0.94$, $p = .350$) nor task-related HRV ($\beta = -0.02$, $t = -0.14$, $p = .886$) contributed significantly to the overall regression model, $F(2,67) = 0.45$, $p = .637$, explaining only 1.3% of the variance in right amygdala-mPFC functional connectivity. Entering the HRV x age interaction term into the model improved the proportion of variance explained in right amygdala-mPFC connectivity ($\Delta R^2 = 0.13$, $F(3,66) = 3.62$, $p = .018$). The interaction between task-related HRV and age significantly predicted right amygdala-mPFC functional connectivity strength ($\beta = 0.86$, $t = 3.14$, $p = .003$). Follow-up regression models indicated that the younger adults appeared to drive this interaction, such that younger adults with higher task-based HRV exhibited significantly weaker right amygdala-mPFC functional connectivity ($\beta = -0.54$, $t = -2.54$, $p = .022$), whereas older adults demonstrated a slight positive, albeit non-significant, association between HRV and right amygdala-mPFC connectivity during the task ($\beta = 0.17$, $t = 1.24$, $p = .222$) (Fig. 2a).

3.2.2. HRV and left amygdala-MPFC functional connectivity

Similar to the right amygdala-mPFC functional connectivity findings, task-related HRV ($\beta = -0.03$, $t = -0.26$, $p = .797$) and age ($\beta = -0.09$, $t = -0.73$, $p = .466$) did not contribute significantly to the overall model, $F(2,67) = 0.27$, $p = .764$, and explained very minimal variance (0.8%) in left amygdala-mPFC functional connectivity strength. However, when the HRV x age interaction term was entered into the model, this slightly improved the proportion of variance explained in left amygdala-mPFC connectivity ($\Delta R^2 = 0.08$), although the overall model remained non-significant, $F(3,66) = 2.07$, $p = .112$. The HRV x age interaction was found to predict left amygdala-mPFC connectivity strength ($\beta = 0.67$, $t = 2.38$, $p = .020$). Follow-up regression models per age group revealed younger adults to drive this significant interaction, whereby greater task-based HRV significantly predicted weaker left amygdala-mPFC functional connectivity in younger adults ($\beta = -0.51$, $t = -2.37$, $p = .031$). Conversely, a non-significant, weak positive association between task-related HRV and left amygdala-mPFC connectivity strength was observed in older adults ($\beta = 0.10$, $t = 0.74$, $p = .461$) (Fig. 2b).[7]

3.3. Whole-Brain functional connectivity analyses

3.3.1. Right amygdala whole-brain functional connectivity

Significant clusters surviving correction as a main effect of HRV for the right amygdala whole-brain functional connectivity analyses are displayed in Table 2. Across adults in both the older and younger age groups, higher task-related HRV was associated with weaker right amygdala connectivity between the right angular gyrus (extending into right superior lateral occipital cortex), and bilateral posterior cingulate gyrus

that task events were not modelled in the present study, the findings reported here have been derived from analyses on the full dataset that formed part of a previous study (Lloyd et al., 2021). Using FSL's FeatQuery, the average % change in amygdala signal between the different regulatory conditions was extracted for left and right amygdala respectively (amygdala seed regions were the same as those adopted in the functional connectivity analyses in the present study). One-sample t-tests were conducted on the amygdala reactivity difference scores between regulatory conditions against zero. Following a similar pattern to self-reported negative emotional intensity, there was a significant change in amygdala reactivity between enhance (increase) and maintain (attend) conditions while responding to negative images across older and younger adults (for right amygdala: $t(69) = 3.67$, $p < .001$, $d = 0.44$; for left amygdala: $t(69) = 2.50$, $p = .015$, $d = 0.30$), in which right and left amygdala activation was greater after enhance relative to maintain, thus suggesting effective up-regulation, particularly of the right amygdala. No significant difference in amygdala activation emerged for suppress (decrease) relative to maintain in response to negative images (right amygdala: $t(69) = 0.60$, $p = .548$, $d = 0.07$; left amygdala: $t(69) = -0.12$, $p = .904$, $d = -0.01$), therefore no significant down-regulation of right or left amygdala reactivity was observed following the suppress regulatory instruction. For enhance relative to suppress in response to negative images, there was a significant difference in amygdala reactivity in which amygdala activation was significantly greater after enhance versus suppress across older and younger adults (right amygdala: $t(69) = 3.58$, $p < .001$, $d = 0.43$; left amygdala: $t(69) = 2.72$, $p = .008$, $d = 0.33$).

[7] Average FD values (across the four task runs) derived from the realignment parameters following MCFLIRT (natural log-transformed to correct for non-normal distribution, Shapiro-Wilk $p < .001$) and a FD by age interaction were not found to significantly predict either right or left amygdala-mPFC functional connectivity strength and therefore do not change the nature of the findings reported here (data not shown).

Table 2
Neural Regions and Local Maxima for Right Amygdala Whole-Brain Connectivity.

Region	H	Cluster Size	BA	MNI Coordinates x	y	z	Z
HRV + (older and younger adults)							
No significant results							
HRV - (older and younger adults)							
Angular Gyrus extending into Superior Lateral Occipital Cortex	R	103	39	40	−58	16	5.89
White Matter	R			36	−52	10	4.27
Superior Lateral Occipital Cortex	R			56	−66	24	3.30
Posterior Cingulate Gyrus	R	87	23	6	−40	32	5.12
	R			2	−42	34	4.59
	L			0	−38	26	4.29
	R/L			0	−40	30	4.06
	L			−4	−48	34	3.59
HRV x Age Interaction + (older and younger adults)							
No significant results							
HRV x Age Interaction – (older and younger adults)							
No significant results							
HRV + (older adults)							
Inferior Frontal Gyrus	R	111	46	46	32	14	4.16
	R			52	34	10	3.82
Frontal Pole	R			48	44	2	3.76
	R			58	38	12	3.76
Inferior Frontal Gyrus	R		45	54	24	12	3.49
	R		44	52	20	12	3.25
HRV - (older adults)							
Superior Lateral Occipital Cortex extending into Angular Gyrus	L	359	39	−38	−62	46	4.86
	L			−36	−76	36	4.43
	L			−36	−70	34	4.35
Supramarginal Gyrus	L			−50	−46	46	4.33
Angular Gyrus extending into Supramarginal Gyrus	L			−44	−48	38	4.26
	L			−44	−54	44	4.24
Precuneus	R/L	159	7	2	−74	60	5.41
	R/L			0	−64	48	3.90
Superior Lateral Occipital Cortex	R			10	−78	54	3.33

Neural regions that demonstrated associations with right amygdala as a function of task-related HRV ($Z = 3.1$; cluster significance: $p < .05$, corrected). Local maxima are listed for clusters containing more than one peak. Cluster size refers to the number of voxels contained within a specific cluster. Coordinates (MNI space) represent location of clusters and their maximum Z-scores (bold) and the location of local maxima within significant clusters and their associated Z-statistic. The Harvard Oxford Structural Cortical and Subcortical atlases within FSL were used to label significant clusters. BA refers to the Brodmann Area for each cluster. The 'R' package *label4MRI* (v1.2) was used to generate the BA label based on the MNI coordinates. *H* = hemisphere (*L* = left, *R* = right).

($Z > 3.1$, $p = 0.05$-corrected). A scatterplot displaying beta values extracted from the bilateral posterior cingulate gyrus cluster with task-based HRV are displayed in Fig. 3. No other clusters survived correction for the positive HRV contrast, nor for positive or negative HRV by age interaction contrasts across the whole sample.

Repeating this analysis in the older adult sample only, a significant main effect of HRV emerged, such that higher task-related HRV was positively correlated with stronger functional connectivity between the right amygdala and the right inferior frontal gyrus, a cluster forming part of the right ventrolateral prefrontal cortex (vlPFC). A scatterplot displaying beta values extracted from this right vlPFC cluster with task-based HRV are displayed in Fig. 3. Moreover, for the HRV negative contrast, higher task-related HRV was associated with weaker right amygdala connectivity with several regions, including bilateral superior lateral occipital cortex extending into left angular and supramarginal gyrus, and bilateral precuneus.

3.3.2. Left amygdala whole-brain functional connectivity

No significant clusters survived correction as a function of HRV for left amygdala functional connectivity in the whole sample ($Z > 3.1$, $p = 0.05$-corrected), suggesting that task-based HRV did not covary with left amygdala whole-brain functional connectivity across older and younger adults throughout the reappraisal task.

When the left amygdala voxelwise whole-brain search was restricted to adults in the older age sample, a significant positive main effect of HRV was observed, in which higher task-related HRV was correlated with stronger left amygdala connectivity with the right inferior frontal gyrus (vlPFC) and more extensively with the right precentral gyrus ($Z > 3.1$, $p = 0.05$-corrected). Furthermore, significant clusters also survived correction for the negative HRV contrast, such that higher task-based HRV correlated with reduced left amygdala – left lateral occipital cortex connectivity. Other brain regions that survived correction as a main effect of HRV for the left amygdala whole-brain functional connectivity analyses in the older adults are displayed in Table 3.

3.3.3. MPFC whole-brain functional connectivity

No clusters survived correction as a main effect of HRV for the mPFC seed in a voxelwise whole-brain search in the whole sample, nor when the analysis was restricted to adults in the older age group ($Z > 3.1$, $p = 0.05$-corrected). Therefore, task-related HRV did not significantly predict functional connectivity of this particular area of the mPFC during reappraisal.

4. Discussion

The principal aim of the present study was to examine the relationship between HRV and neural functional connectivity whilst older and younger adults engaged in a voluntary emotion regulation task. Based on the NIM (Smith et al., 2017; Thayer and Lane, 2000, 2009), we hypothesised that higher task-related HRV would be positively associated with stronger functional coupling between the amygdala and mPFC in an active regulatory context. In older adults, we observed a slight positive, but

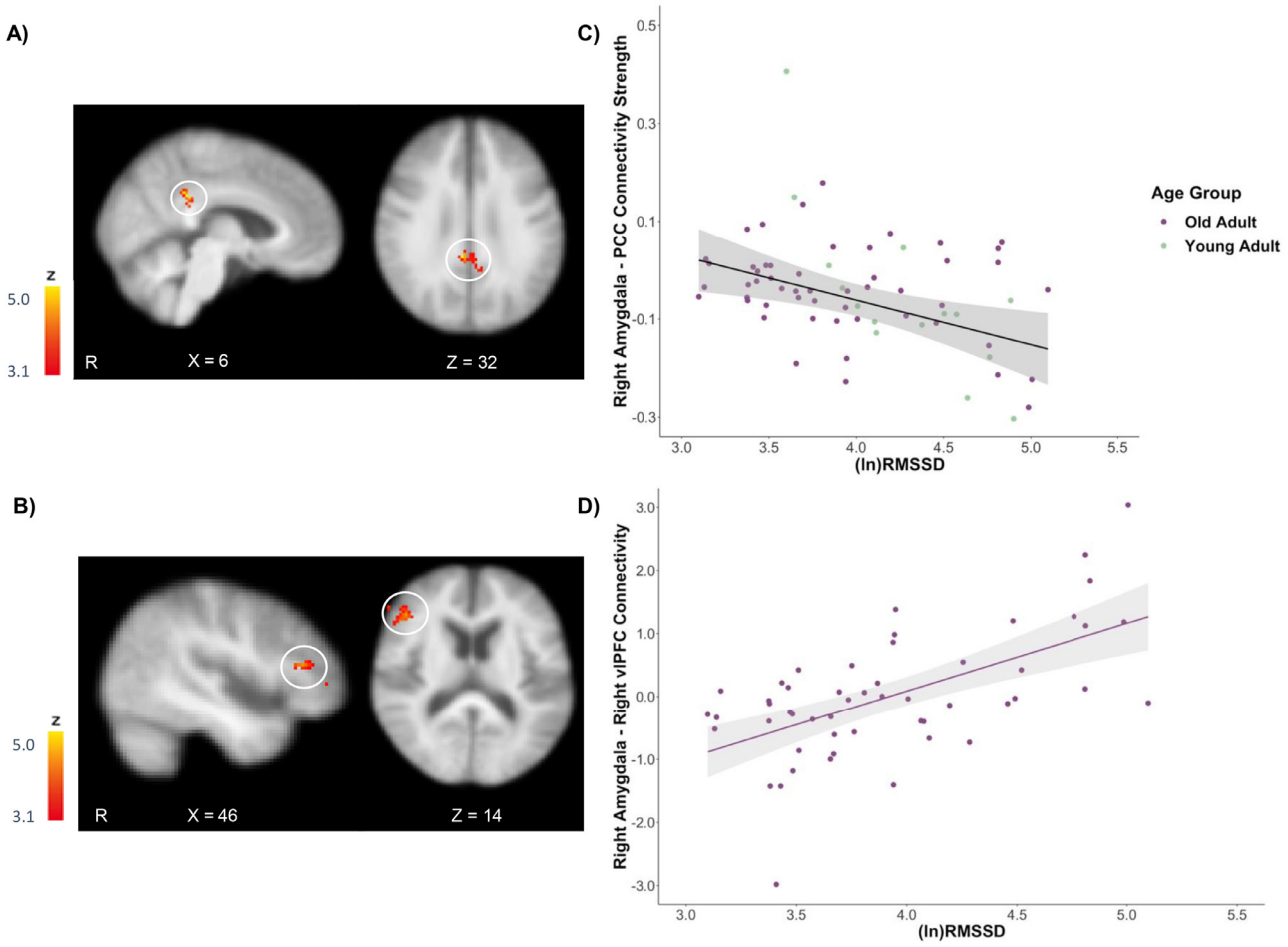

Fig. 3. (A) Significant bilateral PCC cluster that survived correction as a main effect for the negative HRV contrast in the right amygdala whole-brain analysis ($Z > 3.1$, $p = 0.05$-corrected). (B) Significant right inferior frontal gyrus (vlPFC) cluster that survived correction as a main effect for the positive HRV contrast in the right amygdala whole-brain analysis restricted to the older adult sample ($Z > 3.1$, $p = 0.05$-corrected). (C) Scatterplot displays the inverse association between task-based HRV ((ln)RMSSD) values and standardised beta values depicting right amygdala-bilateral PCC connectivity strength in the whole sample during the reappraisal task in older and younger adults ($N = 70$). Note that the different colours assigned to older (purple) versus younger (light green) adult age groups are depicted for display purposes only. (D) Scatterplot displays the positive association between task-related HRV ((ln)RMSSD) values and standardised beta values depicting right amygdala–right vlPFC connectivity strength in the older adult sample (controlling for age). *PCC, posterior cingulate cortex; HRV, heart rate variability; vlPFC, ventrolateral prefrontal cortex; (ln)RMSSD, natural* log *transformed root mean square of successive differences.*

non-significant, association between HRV and amygdala-mPFC connectivity. Conversely, younger adults displayed a stronger, inverse association, whereby higher task-related HRV was linked to reduced functional connectivity between the amygdala and mPFC. Furthermore, in a voxelwise whole-brain search, we discovered that older and younger adults with higher task-based HRV exhibited weaker right amygdala-PCC connectivity. Interestingly, in older adults, higher HRV during reappraisal was associated with stronger coupling between the right amygdala and right vlPFC. Our findings indicate that task-related HRV covaries with amygdala functional connectivity during emotion regulation, and more crucially highlight the importance of assessing both HRV and brain function during an active emotion regulatory context.

Functional connectivity between the amygdala and mPFC is proposed to support adaptive emotion regulation, with resting HRV posited to serve as a peripheral index of prefrontal inhibitory control (Thayer and Lane, 2000, 2009; Thayer et al., 2009a). In line with this proposition, prior studies have reported positive associations between resting HRV and amygdala-mPFC connectivity strength irrespective of age (Nashiro et al., 2022; Sakaki et al., 2016). However, within the context of the emotion regulation task, we found significant interactions between age and task-related HRV to predict both right and left amygdala coupling with the mPFC. The direction of the effect was unexpected, with the younger adults driving the interaction, but in whom higher task-based HRV was linked to weaker, rather than a strong positive, coupling between the amygdala and mPFC. Medial prefrontal areas have been suggested to support automatic/implicit emotion regulation, while lateral regions of the prefrontal cortex have been implicated in explicit or voluntary emotion regulatory processes requiring greater cognitive control (Braunstein et al., 2017; Phillips et al., 2008). Moreover, the mPFC has been classified as one of the main nodes of the default mode network (DMN), a neural hub underlying introspective-related mental processes during rest, including emotional and self-referential processing (Andrews-Hanna et al., 2010; Buckner and Carroll, 2007; Raichle et al., 2001). Regions comprising the DMN are generally suppressed while actively engaging in cognitive tasks (Raichle et al., 2001). It is therefore likely that this particular region of the mPFC is more heavily recruited during rest compared to an active task context that requires individuals to reappraise. Thus, prior findings indicating stronger resting amygdala-mPFC connectivity as a function of higher resting HRV may reflect more implicit/automatic emotion regulation in the absence of an emotion regulation task that targets more explicit/controlled regulatory processes (Braunstein et al., 2017; Sakaki et al., 2016). Indeed, during rest, we found a sub-threshold cluster within the mPFC close to our ROI that demonstrated increased functional connectivity with

Table 3
Neural Regions and Local Maxima for Left Amygdala Whole-Brain Connectivity.

Region	H	Cluster Size	BA	MNI Coordinates x	y	z	Z
HRV + (older and younger adults)							
No significant results							
HRV - (older and younger adults)							
No significant results							
HRV x Age Interaction + (older and younger adults)							
No significant results							
HRV x Age Interaction – (older and younger adults)							
No significant results							
HRV + (older adults)							
Inferior Frontal Gyrus	R	78	44	48	12	30	4.10
Precentral Gyrus	R		6	38	0	32	3.99
Precentral Gyrus extending into Middle Frontal Gyrus	R		8	44	8	34	3.71
Precentral Gyrus	R		6	46	4	28	3.65
	R			48	6	32	3.39
	R		8	32	0	34	3.28
HRV - (older adults)							
Superior Lateral Occipital Cortex	L	156	39	−42	−68	44	4.25
	L			−48	−78	36	4.14
	L			−38	−68	40	3.87
	L			−40	−70	36	3.83
Angular Gyrus	L			−44	−56	46	3.66
Angular Gyrus extending into Posterior Supramarginal Gyrus	L			−48	−52	42	3.59

Neural regions that demonstrated associations with left amygdala as a function of task-related HRV ($Z = 3.1$; cluster significance: $p < .05$, corrected). Local maxima are listed for clusters containing more than one peak. Cluster size refers to the number of voxels contained within a specific cluster. Coordinates (MNI space) represent location of clusters and their maximum Z-scores (bold) and the location of local maxima within significant clusters and their associated Z-statistic. The Harvard Oxford Structural Cortical and Subcortical atlases within FSL were used to label significant clusters. BA refers to the Brodmann Area for each cluster. The 'R' package *label4MRI* (v1.2) was used to generate the BA label based on the MNI coordinates. *H* = hemisphere (*L* = left, *R* = right).

the left amygdala as a function of higher task-related HRV across older and younger adults (see Figure S3 in the Supplementary Material). Recently, Nashiro et al. (2022) also found that increases in resting HRV via biofeedback were correlated with stronger left, but not right, amygdala coupling with the mPFC at rest. Furthermore, prior work has found inverse amygdala-mPFC coupling when using reappraisal to decrease negative affect in a student-aged population (Lee et al., 2012). Hence, the inverse association reported here in younger adults may be driven by the decrease conditions throughout the task. However, given the short trial durations in the current study, an event-related connectivity analysis would be susceptible to fit too much noise and thus render any findings unreliable. Whilst our findings potentially suggest that the regulatory context can affect both the laterality and directionality of amygdala-mPFC functional connectivity associations with task-based HRV, future work should aim to replicate these findings using a task paradigm with longer trial durations to allow for a more targeted event-related connectivity analysis.

Moreover, higher task-related HRV was significantly associated with weaker right amygdala connectivity between the right angular gyrus and bilateral PCC across the emotion regulation task in both age groups. The angular gyrus and PCC also form major nodes of the DMN (Raichle et al., 2001). Weaker resting-state functional connectivity between the right amygdala and PCC has previously been linked to greater reappraisal success (i.e., effective down-regulation of negative emotion) in younger adults (Uchida et al., 2015), whereas increased amygdala-PCC resting-state functional connectivity has been observed following exposure to an acute stressor (Veer et al., 2011). More recently, Baez-Lugo et al. (2021) reported that greater right amygdala-PCC functional connectivity following exposure to videos containing highly negative emotional content (i.e., people suffering) was significantly correlated with higher rumination, anxiety, and stress in elderly individuals (Baez-Lugo et al., 2021). Critically, those older adults who self-reported more frequent negative thoughts after watching the negative emotional videos were those who also exhibited stronger right amygdala-PCC connectivity. At a trait level, lower resting HRV has been linked to both increased rumination and emotion dysregulation (Visted et al., 2017; Williams et al., 2017). Relatedly, individuals with lower resting HRV have been reported to exhibit phasic HRV suppression in response to fearful distractor stimuli under conditions of both low and high cognitive load, thus displaying an autonomic stress response to relatively trivial threat cues (Park et al., 2014). Conversely, individuals with higher resting HRV appear to exert greater self-regulatory effort as indicated by phasic HRV enhancement in the face of fearful distractors under conditions of low cognitive load, and no presence of phasic HRV suppression under conditions of high cognitive load (Park et al., 2014). Therefore, even under relatively stressful conditions of the task, individuals with higher HRV did not demonstrate an autonomic stress response, whereas those with lower HRV experienced difficulties with engaging self-regulatory processes to effectively cope with task demands. Collectively, the observation of weaker right amygdala-PCC connectivity in older and younger adults with overall elevated task-related HRV in our study may therefore reflect an increased ability to effectively engage with the emotion regulation task at hand.

Finally, we found that older adults with greater task-related HRV exhibited stronger functional connectivity between the amygdala and right vlPFC in a reappraisal context. This finding is particularly interesting since Sakaki et al. (2016) reported a similar association between resting HRV and resting amygdala-vlPFC connectivity in younger, but not older adults, suggesting that younger adults with relatively higher resting HRV were more likely to spontaneously recruit neural regions involved in explicit emotion regulation. Considering empirical evidence that has reported phasic HRV increases to reflect greater self-regulatory effort and emotion regulatory success (Butler et al., 2006; Denson et al., 2011; Segerstrom and Nes, 2007), overall elevated task-related HRV when directly challenged by stimuli designed to elicit negative emotions may also indicate a greater ability to actively engage brain regions underlying successful voluntary emotion regulation. The vlPFC has increasingly been identified as a pivotal neural region involved in

emotion regulatory processes (Wager et al., 2008; Zhao et al., 2021), and is an area in which age-related differences have been reported during reappraisal (Opitz et al., 2012; Winecoff et al., 2011). The vlPFC, and lateral prefrontal cortex more broadly, is particularly vulnerable to structural and functional atrophy in healthy ageing (Fjell et al., 2009; Raz et al., 2004). The present finding suggests that higher task-related HRV in older age, at least in a voluntary emotion regulation context, may support increased engagement, and possibly functional preservation, of lateral prefrontal cortex, specifically the right vlPFC, facilitating effective reappraisal of negative emotions. Although the left vlPFC has been more frequently reported in reappraisal studies (Berboth and Morawetz, 2021; Buhle et al., 2014), involvement of the right vlPFC here may be characterised by dominance of the right hemisphere in supporting inhibitory-related processes for affective, cognitive, and physiological regulation more broadly (Lane et al., 2009; Thayer et al., 2009b, 2012). Irrespective of any laterality, our findings build on the extant literature on prefrontal mechanisms in reappraisal by highlighting that elevated task-related HRV is associated with positive coupling between the amygdala and vlPFC, which may have implications for psychological wellbeing and resilience in later life.

A few important limitations should be considered when interpreting our findings. Our sample comprised a larger pool of adults in the older age relative to the younger age group, leading to an unequal age distribution. Although age was included as a predictor in our regression models, the small sample of younger adults rendered any findings specific to the younger group as possibly spurious and requiring replication in a larger sample. Furthermore, HRV was derived from a finger pulse oximeter whilst participants were lying down in the scanner and whilst engaging in emotion-related tasks, predominantly reappraisal. Both factors have previously been shown to elevate heart rate and HRV (Butler et al., 2006; Cacioppo et al., 1994), and the use of photoplethysmography to derive HRV metrics, especially RMSSD (Schumann et al., 2021b), could have further resulted in an elevated HRV estimate. However, given that HRV metrics tend to demonstrate strong positive correlations across contexts (Heffner et al., 2022; Wang et al., 2009) and resting HRV modulates phasic HRV changes during emotion regulation (Butler et al., 2006; Segerstrom and Nes, 2007), the relative rank order of task-related HRV across subjects in the present study are likely to be similar to those observed outside of the scanner at rest. Additionally, other lifestyle factors known to influence HRV measures, including smoking status, general fitness/activity level, caffeine intake, and body mass index (Hayano et al., al.,1990; Karason et al., 1999; Sammito and Böckelmann, 2016) were not obtained, therefore we cannot rule out the influence of these factors on the current findings. Future research should aim to acquire reliable heart rate recordings to derive HRV metrics both inside and outside of the scanner (Schumann et al., 2021b) and during rest and whilst performing tasks for calculation of phasic HRV changes (reactivity and recovery measures relative to baseline). Relatedly, aggregation of HRV measures across contexts to capture variance that more strongly represents 'trait-like' HRV may also be insightful (see Bertsch et al., 2012).

Whilst our study augments prior findings which have heavily relied on associations between HRV and functional connectivity during rest by assessing heart-brain function in an active emotion regulatory context, the current study and the majority of prior work have typically relied on relatively static functional connectivity techniques. Although a few studies have examined transient HRV changes and functional connectivity using dynamic functional connectivity (dFC) techniques such as the sliding window approach (Chand et al., 2020; Chang et al., 2013; Schumann et al., 2021a), this method is limited by its reliance on arbitrary selection of truncated time windows to assess both functional connectivity and HRV, with the latter particularly affected by the shorter duration of the measurement period (Shaffer and Ginsberg, 2017; Task Force, 1996). It would therefore be fruitful for future research to employ novel and alternative dFC methods that overcome existing constraints (e.g., co-activation pattern analysis; Liu et al., 2013, 2018) to determine associations between HRV and dynamic neural networks underlying adaptive and flexible regulation across the lifespan.

In conclusion, the current study extends prior resting-state findings by highlighting that task-related HRV covaries with amygdala-cortical functional connectivity in the context of a voluntary emotion regulation task. Particularly, the task-based covariation between functional connectivity of amygdala-vlPFC and amygdala-PCC and task-based HRV provide further, and more direct, support of the NIM. Furthermore, the findings support the notion that HRV is linked to neural mechanisms that facilitate adaptive emotion regulation, which could have implications for wellbeing and resilience in later life. Collectively, our findings accentuate the importance of assessing neurovisceral circuitry during active regulatory contexts to further elucidate core neural mechanisms involved in supporting adaptive self-regulation as a function of HRV more broadly.

Declaration of Competing Interest

Declarations of interest: none. The authors declare no conflict of interest.

Credit authorship contribution statement

Emma Tupitsa: Conceptualization, Formal analysis, Writing – original draft. **Ifeoma Egbuniwe:** Conceptualization, Formal analysis. **William K. Lloyd:** Methodology, Software, Formal analysis, Writing – review & editing. **Marta Puertollano:** Formal analysis, Writing – review & editing. **Birthe Macdonald:** Investigation, Writing – review & editing. **Karin Joanknecht:** Investigation. **Michiko Sakaki:** Conceptualization, Writing – review & editing. **Carien M. van Reekum:** Conceptualization, Methodology, Writing – original draft, Supervision, Funding acquisition.

Data availability

The MRI data that support the findings of this study are openly available on OpenNeuro: 10.18112/openneuro.ds002620.v1.0.0. The pulse data, processing and analysis scripts that support this study are openly available on the Open Science Framework (OSF): https://osf.io/6zdph/.

Acknowledgments

The authors would like to thank Karis Colyer Patel and Laura Bucher for their assistance with processing the pulse data, Shan Shen for MRI support and help in MRI data acquisition, and all participants for devoting their time to our research. This research was supported by grants from the Biotechnology and Biological Sciences Research Council (BB/J009539/1 and BB/L02697X/1) awarded to Carien van Reekum.

Supplementary materials

Supplementary material associated with this article can be found, in the online version, at doi:10.1016/j.neuroimage.2023.120136.

References

Agelink, M.W., Malessa, R., Baumann, B., Majewski, T., Akila, F., Zeit, T., Ziegler, D., 2001. Standardized tests of heart rate variability: normal ranges obtained from 309 healthy humans, and effects of age, gender, and heart rate. Clin. Auton. Res. 11 (2), 99–108. doi:10.1007/BF02322053.

Aldao, A., Sheppes, G., Gross, J.J., 2015. Emotion regulation flexibility. Cogn. Ther. Res. 39 (3), 263–278. doi:10.1007/s10608-014-9662-4.

Andrews-Hanna, J.R., Reidler, J.S., Sepulcre, J., Poulin, R., Buckner, R.L., 2010. Functional-anatomic fractionation of the brain's default network. Neuron 65 (4), 550–562. doi:10.1016/j.neuron.2010.02.005.

Appelhans, B.M., Luecken, L.J., 2006. Heart rate variability as an index of regulated emotional responding. Rev. Gen. Psychol. 10 (3), 229–240. doi:10.1037/1089-2680.10.3.229.

Baas, D., Aleman, A., Kahn, R.S., 2004. Lateralization of amygdala activation: a systematic review of functional neuroimaging studies. Brain Res. Rev. 45 (2), 96–103. doi:10.1016/j.brainresrev.2004.02.004.

Baez-Lugo, S., Deza-Araujo, Y.I., Colette, F., Vuilleumier, P., Klimecki, O., Medit-Ageing Research, G., 2021. Exposure to Negative Socio-Emotional Events Induces Sustained Alteration of Resting-State Brain Networks in the Elderly. ResearchSquare [pre-print] doi:10.21203/rs.3.rs-91196/v2.

Beckmann, C.F., Smith, S.M., 2004. Probabilistic independent component analysis for functional magnetic resonance imaging. IEEE Trans. Med. Imaging 23 (2), 137–152. doi:10.1109/TMI.2003.822821.

Benarroch, E.E., 1993. The central autonomic network: functional organization, dysfunction, and perspective. Mayo Clin. Proc. 68 (10), 988–1001. doi:10.1016/S0025-6196(12)62272-1.

Berboth, S., Morawetz, C., 2021. Amygdala-prefrontal connectivity during emotion regulation: a meta-analysis of psychophysiological interactions. Neuropsychologia 153, 107767. doi:10.1016/j.neuropsychologia.2021.107767.

Berntson, G.G., Bigger, J.T., Eckberg, D.L., Grossman, P., Kaufmann, P.G., Malik, M., et al., 1997. Heart rate variability: origins, methods, and interpretive caveats. Psychophysiology 34 (6), 623–648. doi:10.1111/j.1469-8986.1997.tb02140.x.

Bertsch, K., Hagemann, D., Naumann, E., Schächinger, H., Schulz, A., 2012. Stability of heart rate variability indices reflecting parasympathetic activity. Psychophysiology 49 (5), 672–682. doi:10.1111/j.1469-8986.2011.01341.x.

Bolt, T., Nomi, J.S., Bzdok, D., Salas, J.A., Chang, C., Thomas Yeo, B.T., … Keilholz, S.D., 2022. A parsimonious description of global functional brain organization in three spatiotemporal patterns. Nat. Neurosci. 25 (8), 1093–1103. doi:10.1038/s41593-022-01118-1.

Braunstein, L.M., Gross, J.J., Ochsner, K.N., 2017. Explicit and implicit emotion regulation: a multi-level framework. Soc. Cogn. Affect Neurosci. 12 (10), 1545–1557. doi:10.1093/scan/nsx096.

Buckner, R.L., Carroll, D.C., 2007. Self-projection and the brain. Trends Cogn. Sci. 11 (2), 49–57. doi:10.1016/j.tics.2006.11.004, (Regul. Ed.).

Buhle, J.T., Silvers, J.A., Wager, T.D., Lopez, R., Onyemekwu, C., Kober, H., … Ochsner, K.N., 2014. Cognitive reappraisal of emotion: a meta-analysis of human neuroimaging studies. Cereb. Cortex 24 (11), 2981–2990. doi:10.1093/cercor/bht154.

Butler, E.A., Wilhelm, F.H., Gross, J.J., 2006. Respiratory sinus arrhythmia, emotion, and emotion regulation during social interaction. Psychophysiology 43 (6), 612–622. doi:10.1111/j.1469-8986.2006.00467.x.

Cacioppo, J.T., Berntson, G.G., Binkley, P.F., Quigley, K.S., Uchino, B.N., Fieldstone, A., 1994. Autonomic Cardiac Control. II. Noninvasive indices and basal response as revealed by autonomic blockades. Psychophysiology 31 (6), 586–598. doi:10.1111/j.1469-8986.1994.tb02351.x.

Chand, T., Li, M., Jamalabadi, H., Wagner, G., Lord, A., Alizadeh, S., … Sen, Z.D., 2020. Heart rate variability as an index of differential brain dynamics at rest and after acute stress induction. Front. Neurosci. 14, 645. doi:10.3389/fnins.2020.00645.

Chang, C., Metzger, C.D., Glover, G.H., Duyn, J.H., Heinze, H.J., Walter, M., 2013. Association between heart rate variability and fluctuations in resting-state functional connectivity. NeuroImage 68, 93–104. doi:10.1016/j.neuroimage.2012.11.038.

Chen, P.Y., Chiou, J.M., Yang, Y.F., Chen, Y.T., Hsieh, H.L., Chang, Y.L., Tseng, W.Y.I., 2016. Heterogeneous aging effects on functional connectivity in different cortical regions: a resting-state functional MRI study using functional data analysis. PLoS One 11 (9), e0162028. doi:10.1371/journal.pone.0162028.

Cho, J.W., Korchmaros, A., Vogelstein, J.T., Milham, M.P., Xu, T., 2021. Impact of concatenating fMRI data on reliability for functional connectomics. NeuroImage 226, 117549. doi:10.1016/j.neuroimage.2020.117549.

Cole, M.W., Ito, T., Schultz, D., Mill, R., Chen, R., Cocuzza, C., 2019. Task activations produce spurious but systematic inflation of task functional connectivity estimates. NeuroImage 189, 1–18. doi:10.1016/j.neuroimage.2018.12.054.

Cox, R.W., 1996. AFNI: software for analysis and visualization of functional magnetic resonance neuroimages. Comput. Biomed. Res. 29 (3), 162–173. doi:10.1006/cbmr.1996.0014.

Denson, T.F., Grisham, J.R., Moulds, M.L., 2011. Cognitive reappraisal increases heart rate variability in response to an anger provocation. Motiv. Emot. 35 (1), 14–22. doi:10.1007/s11031-011-9201-5.

Etkin, A., Egner, T., Kalisch, R., 2011. Emotional processing in anterior cingulate and medial prefrontal cortex. Trends Cogn. Sci. 15 (2), 85–93. doi:10.1016/j.tics.2010.11.004, (Regul. Ed.).

Finn, E.S., 2021. Is it time to put rest to rest? Trends Cogn. Sci. 25 (12), 1021–1032. doi:10.1016/j.tics.2021.09.005, (Regul. Ed.).

Finn, E.S., Bandettini, P.A., 2021. Movie-watching outperforms rest for functional connectivity-based prediction of behavior. NeuroImage 235, 117963. doi:10.1016/j.neuroimage.2021.117963.

Fjell, A.M., Westlye, L.T., Amlien, I., Espeseth, T., Reinvang, I., Raz, N., … Walhovd, K.B., 2009. High consistency of regional cortical thinning in aging across multiple samples. Cereb. Cortex 19 (9), 2001–2012. doi:10.1093/cercor/bhn232.

Gorgolewski, K.J., Lurie, D., Urchs, S., Kipping, J.A., Craddock, R.C., Milham, M.P., … Smallwood, J., 2014. A correspondence between individual differences in the brain's intrinsic functional architecture and the content and form of self-generated thoughts. PLoS One 9 (5), e97176. doi:10.1371/journal.pone.0097176.

Griffanti, L., Douaud, G., Bijsterbosch, J., Evangelisti, S., Alfaro-Almagro, F., Glasser, M.F., … Smith, S.M., 2017. Hand classification of fMRI ICA noise components. NeuroImage 154, 188–205. doi:10.1016/j.neuroimage.2016.12.036.

Gross, J.J., John, O.P., 2003. Individual differences in two emotion regulation processes: implications for affect, relationships, and well-being. J. Pers. Soc. Psychol. 85 (2), 348–362. doi:10.1037/0022-3514.85.2.348.

Grossman, P., Taylor, E.W., 2007. Toward understanding respiratory sinus arrhythmia: relations to cardiac vagal tone, evolution and biobehavioral functions. Biol. Psychol. 74 (2), 263–285. doi:10.1016/j.biopsycho.2005.11.014.

Hayano, J., Yamada, M., Sakakibara, Y., Fujinami, T., Yokoyama, K., Watanabe, Y., Takata, K., 1990. Short-and long-term effects of cigarette smoking on heart rate variability. Am. J. Cardiol. 65 (1), 84–88. doi:10.1016/0002-9149(90)90030-5.

Heffner, K.L., Quinones, M.M., Gallegos, A.M., Crean, H.F., Lin, F., Suhr, J.A., 2022. Subjective memory in adults over 50 years of age: associations with affective and physiological markers of emotion regulation. Aging Ment. Health 26 (5), 971–979. doi:10.1080/13607863.2021.1904829.

Hill, L.K., Siebenbrock, A., Sollers, J.J., Thayer, J.F., 2009. Are all measures created equal? Heart rate variability and respiration. Biomed. Sci. Instrum. 45, 71–76.

Ingjaldsson, J.T., Laberg, J.C., Thayer, J.F., 2003. Reduced heart rate variability in chronic alcohol abuse: relationship with negative mood, chronic thought suppression, and compulsive drinking. Biol. Psychiatry 54 (12), 1427–1436. doi:10.1016/S0006-3223(02)01926-1.

Jenkinson, M., Bannister, P., Brady, M., Smith, S., 2002. Improved optimization for the robust and accurate linear registration and motion correction of brain images. NeuroImage 17 (2), 825–841. doi:10.1016/s1053-8119(02)91132-8.

Jenkinson, M., Beckmann, C.F., Behrens, T.E., Woolrich, M.W., Smith, S.M., 2012. FSL. NeuroImage 62 (2), 782–790. doi:10.1016/j.neuroimage.2011.09.015.

Karason, K., Mølgaard, H., Wikstrand, J., Sjöström, L., 1999. Heart rate variability in obesity and the effect of weight loss. Am. J. Cardiol. 83 (8), 1242–1247. doi:10.1016/S0002-9149(99)00066-1.

Kleiger, R.E., Stein, P.K., Bigger, J.T., 2005. Heart rate variability: measurement and clinical utility. Ann. Noninvasive Electrocardiol. 10 (1), 88–101. doi:10.1111/j.1542-474X.2005.10101.x.

Kogan, A., Gruber, J., Shallcross, A.J., Ford, B.Q., Mauss, I.B., 2013. Too much of a good thing? Cardiac vagal tone's nonlinear relationship with well-being. Emotion 13 (4), 599–604. doi:10.1037/a0032725.

Kumral, D., Schaare, H.L., Beyer, F., Reinelt, J., Uhlig, M., Liem, F., … Gaebler, M., 2019. The age-dependent relationship between resting heart rate variability and functional brain connectivity. NeuroImage 185, 521–533. doi:10.1016/j.neuroimage.2018.10.027.

Laborde, S., Mosley, E., Mertgen, A., 2018. Vagal tank theory: the three RS of cardiac vagal control functioning–resting, reactivity, and recovery. Front. Neurosci. 12, 458. doi:10.3389/fnins.2018.00458.

Lane, R.D., McRae, K., Reiman, E.M., Chen, K., Ahern, G.L., Thayer, J.F., 2009. Neural correlates of heart rate variability during emotion. NeuroImage 44 (1), 213–222. doi:10.1016/j.neuroimage.2008.07.056.

Lane, R.D., Weidenbacher, H., Smith, R., Fort, C., Thayer, J.F., Allen, J.J., 2013. Subgenual anterior cingulate cortex activity covariation with cardiac vagal control is altered in depression. J. Affect. Disord. 150 (2), 565–570. doi:10.1016/j.jad.2013.02.005.

Lang, P.J., Bradley, M.M., Cuthbert, B.N., 2008. International Affective Picture System (IAPS): Affective Ratings of Pictures and Instruction Manual. University of Florida, Gainesville, FL (Technical Report A-8).

Lee, H., Heller, A.S., Van Reekum, C.M., Nelson, B., Davidson, R.J., 2012. Amygdala–prefrontal coupling underlies individual differences in emotion regulation. NeuroImage 62 (3), 1575–1581. doi:10.1016/j.neuroimage.2012.05.044.

Lehrer, P.M., Gevirtz, R., 2014. Heart rate variability biofeedback: how and why does it work? Front. Psychol. 756. doi:10.3389/fpsyg.2014.00756.

Li, J., Kong, R., Liégeois, R., Orban, C., Tan, Y., Sun, N., … Yeo, B.T., 2019. Global signal regression strengthens association between resting-state functional connectivity and behavior. NeuroImage 196, 126–141. doi:10.1016/j.neuroimage.2019.04.016.

Liu, X., Chang, C., Duyn, J.H., 2013. Decomposition of spontaneous brain activity into distinct fMRI co-activation patterns. Front. Syst. Neurosci. 7, 101. doi:10.3389/fnsys.2013.00101.

Liu, X., Zhang, N., Chang, C., Duyn, J.H., 2018. Co-activation patterns in resting-state fMRI signals. NeuroImage 180, 485–494. doi:10.1016/j.neuroimage.2018.01.041.

Lloyd, W.K., Morriss, J., Macdonald, B., Joanknecht, K., Nihouarn, J., Van Reekum, C.M., 2021a. Longitudinal change in executive function is associated with impaired top-down frontolimbic regulation during reappraisal in older adults. NeuroImage 225, 117488. doi:10.1016/j.neuroimage.2020.117488.

Lloyd, W.K., Morriss, J., Macdonald, B., Joanknecht, K., Nihouarn, J., Van Reekum, C.M., 2021b. Emotion Regulation in the Ageing Brain, University of Reading, BBSRC. OpenNeuro Version 1 doi:10.18112/openneuro.ds002620.v1.0.0.

Maier, S.U., Hare, T.A., 2017. Higher heart-rate variability is associated with ventromedial prefrontal cortex activity and increased resistance to temptation in dietary self-control challenges. J. Neurosci. 37 (2), 446–455. doi:10.1523/JNEUROSCI.2815-16.2016.

Mather, M., Thayer, J.F., 2018. How heart rate variability affects emotion regulation brain networks. Curr. Opin. Behav. Sci. 19, 98–104. doi:10.1016/j.cobeha.2017.12.017.

Mayer, A.R., Ling, J.M., Dodd, A.B., Shaff, N.A., Wertz, C.J., Hanlon, F.M., 2019. A comparison of denoising pipelines in high temporal resolution task-based functional magnetic resonance imaging data. Hum. Brain Mapp. 40 (13), 3843–3859. doi:10.1002/hbm.24635.

Morawetz, C., Riedel, M.C., Salo, T., Berboth, S., Eickhoff, S.B., Laird, A.R., Kohn, N., 2020. Multiple large-scale neural networks underlying emotion regulation. Neurosci. Biobehav. Rev. 116, 382–395. doi:10.1016/j.neubiorev.2020.07.001.

Murphy, K., Birn, R.M., Handwerker, D.A., Jones, T.B., Bandettini, P.A., 2009. The impact of global signal regression on resting state correlations: are anti-correlated networks introduced? NeuroImage 44 (3), 893–905. doi:10.1016/j.neuroimage.2008.09.036.

Murphy, K., Fox, M.D., 2017. Towards a consensus regarding global signal regression for resting state functional connectivity MRI. NeuroImage 154, 169–173. doi:10.1016/j.neuroimage.2016.11.052.

Nashiro, K., Min, J., Yoo, H.J., Cho, C., Bachman, S.L., Dutt, S., … Mather, M., 2022. Increasing coordination and responsivity of emotion-related brain regions with a heart rate variability biofeedback randomized trial. Cogn. Affect. Behav. Neurosci. 1–18. doi:10.3758/s13415-022-01032-w.

Nebel, M.B., Lidstone, D.E., Wang, L., Benkeser, D., Mostofsky, S.H., Risk, B.B., 2022. Accounting for motion in resting-state fMRI: what part of the spectrum are we characterizing in autism spectrum disorder? NeuroImage 257, 119296. doi:10.1016/j.neuroimage.2022.119296.

Nomi, J., Bzdok, D., Li, J., Bolt, T., Kornfeld, S., Goodman, Z., … & Uddin, L. (2022). Global Signal Topography in the Human Brain Differs Systematically Across the Lifespan. bioRxiv. [pre-print]. 10.1101/2022.07.27.501804

Opitz, P.C., Rauch, L.C., Terry, D.P., Urry, H.L., 2012. Prefrontal mediation of age differences in cognitive reappraisal. Neurobiol. Aging 33 (4), 645–655. doi:10.1016/j.neurobiolaging.2010.06.004.

Park, G., Vasey, M.W., Van Bavel, J.J., Thayer, J.F., 2014. When tonic cardiac vagal tone predicts changes in phasic vagal tone: the role of fear and perceptual load. Psychophysiology 51 (5), 419–426. doi:10.1111/PSYP.12186.

Pham, D., McDonald, D., Ding, L., Nebel, M.B., Mejia, A., 2023. Less is more: balancing noise reduction and data retention in fMRI with data-driven scrubbing. NeuroImage, 119972 doi:10.1016/j.neuroimage.2023.119972.

Phillips, M.L., Ladouceur, C.D., Drevets, W.C., 2008. A neural model of voluntary and automatic emotion regulation: implications for understanding the pathophysiology and neurodevelopment of bipolar disorder. Mol. Psychiatry 13 (9), 833–857. doi:10.1038/mp.2008.65.

Porges, S.W., 2007. The polyvagal perspective. Biol. Psychol. 74 (2), 116–143. doi:10.1016/j.biopsycho.2006.06.009.

Porges, S.W., 2011. The Polyvagal Theory: Neurophysiological Foundations of Emotions, Attachment, Communication, and Self-Regulation (Norton Series On Interpersonal Neurobiology). WW Norton & Company.

Power, J.D., Barnes, K.A., Snyder, A.Z., Schlaggar, B.L., Petersen, S.E., 2012. Spurious but systematic correlations in functional connectivity MRI networks arise from subject motion. NeuroImage 59 (3), 2142–2154. doi:10.1016/j.neuroimage.2011.10.018.

Raichle, M.E., MacLeod, A.M., Snyder, A.Z., Powers, W.J., Gusnard, D.A., Shulman, G.L., 2001. A default mode of brain function. Proc. Natl Acad. Sci. 98 (2), 676–682. doi:10.1073/pnas.98.2.676.

Raz, N., Gunning-Dixon, F., Head, D., Rodrigue, K.M., Williamson, A., Acker, J.D., 2004. Aging, sexual dimorphism, and hemispheric asymmetry of the cerebral cortex: replicability of regional differences in volume. Neurobiol. Aging 25 (3), 377–396. doi:10.1016/S0197-4580(03)00118-0.

Russoniello, C.V., Zhirnov, Y.N., Pougatchev, V.I., Gribkov, E.N., 2013. Heart rate variability and biological age: implications for health and gaming. Cyberpsychol. Behav. Soc. Netw. 16 (4), 302–308. doi:10.1089/cyber.2013.1505.

Sakaki, M., Nga, L., Mather, M., 2013. Amygdala functional connectivity with medial prefrontal cortex at rest predicts the positivity effect in older adults' memory. J. Cogn. Neurosci. 25 (8), 1206–1224. doi:10.1162/jocn_a_00392.

Sakaki, M., Yoo, H.J., Nga, L., Lee, T.H., Thayer, J.F., Mather, M., 2016. Heart rate variability is associated with amygdala functional connectivity with MPFC across younger and older adults. NeuroImage 139, 44–52. doi:10.1016/j.neuroimage.2016.05.076.

Sammito, S., Böckelmann, I., 2016. Factors influencing heart rate variability. Int. Cardiovas. Forum J. 6, 18–22. doi:10.17987/icfj.v6i0.242.

Schumann, A., De La Cruz, F., Köhler, S., Brotte, L., Bär, K.J., 2021a. The influence of heart rate variability biofeedback on cardiac regulation and functional brain connectivity. Front. Neurosci. 15, 775. doi:10.3389/fnins.2021.691988.

Schumann, A., Suttkus, S., Bär, K.J., 2021b. Estimating resting HRV during fMRI: a comparison between laboratory and scanner environment. Sensors 21 (22), 7663. doi:10.3390/s21227663.

Segerstrom, S.C., Nes, L.S., 2007. Heart rate variability reflects self-regulatory strength, effort, and fatigue. Psychol. Sci. 18 (3), 275–281. doi:10.1111/j.1467-9280.2007.01888.x.

Shaffer, F., Ginsberg, J.P., 2017. An overview of heart rate variability metrics and norms. Front. Public Health 5, 258. doi:10.3389/fpubh.2017.00258.

Smallwood, J., Schooler, J.W., 2015. The science of mind wandering: empirically navigating the stream of consciousness. Annu. Rev. Psychol. 66, 487–518. doi:10.1146/annurev-psych-010814-015331.

Smith, R., Thayer, J.F., Khalsa, S.S., Lane, R.D., 2017. The hierarchical basis of neurovisceral integration. Neurosci. Biobehav. Rev. 75, 274–296. doi:10.1016/j.neubiorev.2017.02.003.

Smith, S.M., 2002. Fast robust automated brain extraction. Hum. Brain Mapp. 17 (3), 143–155. doi:10.1002/hbm.10062.

Smith, S.M., Jenkinson, M., Woolrich, M.W., Beckmann, C.F., Behrens, T.E., Johansen-Berg, H., … Matthews, P.M., 2004. Advances in functional and structural MR image analysis and implementation as FSL. NeuroImage 23, S208–S219. doi:10.1016/j.neuroimage.2004.07.051.

Steinfurth, E.C., Wendt, J., Geisler, F., Hamm, A.O., Thayer, J.F., Koenig, J., 2018. Resting state vagally-mediated heart rate variability is associated with neural activity during explicit emotion regulation. Front. Neurosci. 12, 794. doi:10.3389/fnins.2018.00794.

Tagliazucchi, E., Laufs, H., 2014. Decoding wakefulness levels from typical fmri resting-state data reveals reliable drifts between wakefulness and sleep. Neuron 82 (3), 695–708. doi:10.1016/j.neuron.2014.03.020.

Tarvainen, M.P., Niskanen, J.P., Lipponen, J.A., Ranta-Aho, P.O., Karjalainen, P.A., 2014. Kubios HRV–Heart rate variability analysis software. Comput. Methods Program. Biomed. 113 (1), 210–220. doi:10.1016/j.cmpb.2013.07.024.

Task Force of the European Society of Cardiology, 1996. Heart rate variability: standards of measurement, physiological interpretation and clinical use. Circulation 93, 1043–1065.

Thayer, J.F., Åhs, F., Fredrikson, M., Sollers III, J.J., Wager, T.D, 2012. A meta-analysis of heart rate variability and neuroimaging studies: implications for heart rate variability as a marker of stress and health. Neurosci. Biobehav. Rev. 36 (2), 747–756. doi:10.1016/j.neubiorev.2011.11.009.

Thayer, J.F., Hansen, A.L., Saus-Rose, E., Johnsen, B.H., 2009a. Heart rate variability, prefrontal neural function, and cognitive performance: the neurovisceral integration perspective on self-regulation, adaptation, and health. Ann. Behav. Med. 37 (2), 141–153. doi:10.1007/s12160-009-9101-z.

Thayer, J.F., Lane, R.D., 2000. A model of neurovisceral integration in emotion regulation and dysregulation. J. Affect. Disord. 61 (3), 201–216. doi:10.1016/S0165-0327(00)00338-4.

Thayer, J.F., Lane, R.D., 2009. Claude Bernard and the heart–brain connection: further elaboration of a model of neurovisceral integration. Neurosci. Biobehav. Rev. 33 (2), 81–88. doi:10.1016/j.neubiorev.2008.08.004.

Thayer, J.F., Sollers, J.J., Labiner, D.M., Weinand, M., Herring, A.M., Lane, R.D., Ahern, G.L, 2009b. Age-related differences in prefrontal control of heart rate in humans: a pharmacological blockade study. Int. J. Psychophysiol. 72 (1), 81–88. doi:10.1016/j.ijpsycho.2008.04.007.

Thompson, R.A., 1994. Emotion regulation: a theme in search of definition. Monogr. Soc. Res. Child Dev. 59 (2/3), 25–52. doi:10.2307/1166137.

Uchida, M., Biederman, J., Gabrieli, J.D., Micco, J., de Los Angeles, C., Brown, A., … Whitfield-Gabrieli, S., 2015. Emotion regulation ability varies in relation to intrinsic functional brain architecture. Soc. Cogn. Affect. Neurosci. 10 (12), 1738–1748. doi:10.1093/scan/nsv059.

Uddin, L.Q., 2017. Mixed signals: on separating brain signal from noise. Trends Cogn. Sci. 21 (6), 405–406. doi:10.1016/j.tics.2017.04.002, (Regul. Ed.).

van Reekum, C.M., Johnstone, T., Urry, H.L., Thurow, M.E., Schaefer, H.S., Alexander, A.L., Davidson, R.J., 2007. Gaze fixations predict brain activation during the voluntary regulation of picture-induced negative affect. NeuroImage 36 (3), 1041–1055. doi:10.1016/j.neuroimage.2007.03.052.

Veer, I.M., Oei, N.Y., Spinhoven, P., van Buchem, M.A., Elzinga, B.M., Rombouts, S.A., 2011. Beyond acute social stress: increased functional connectivity between amygdala and cortical midline structures. NeuroImage 57 (4), 1534–1541. doi:10.1016/j.neuroimage.2011.05.074.

Visted, E., Sørensen, L., Osnes, B., Svendsen, J.L., Binder, P.E., Schanche, E., 2017. The association between self-reported difficulties in emotion regulation and heart rate variability: the salient role of not accepting negative emotions. Front. Psychol. 8, 328. doi:10.3389/fpsyg.2017.00328.

Wager, T.D., Davidson, M.L., Hughes, B.L., Lindquist, M.A., Ochsner, K.N., 2008. Prefrontal-subcortical pathways mediating successful emotion regulation. Neuron 59 (6), 1037–1050. doi:10.1016/j.neuron.2008.09.006.

Wang, X., Ding, X., Su, S., Li, Z., Riese, H., Thayer, J.F., … Snieder, H., 2009. Genetic influences on heart rate variability at rest and during stress. Psychophysiology 46 (3), 458–465. doi:10.1111/j.1469-8986.2009.00793.x.

Williams, D.P., Feeling, N.R., Hill, L.K., Spangler, D.P., Koenig, J., Thayer, J.F., 2017. Resting heart rate variability, facets of rumination and trait anxiety: implications for the perseverative cognition hypothesis. Front. Hum. Neurosci. 11, 520. doi:10.3389/fnhum.2017.00520.

Winecoff, A., LaBar, K.S., Madden, D.J., Cabeza, R., Huettel, S.A., 2011. Cognitive and neural contributors to emotion regulation in aging. Soc. Cogn. Affect Neurosci. 6 (2), 165–176. doi:10.1093/scan/nsq030.

Woolrich, M.W., Behrens, T.E., Beckmann, C.F., Jenkinson, M., Smith, S.M., 2004. Multilevel linear modelling for FMRI group analysis using Bayesian inference. NeuroImage 21 (4), 1732–1747. doi:10.1016/j.neuroimage.2003.12.023.

Woolrich, M.W., Jbabdi, S., Patenaude, B., Chappell, M., Makni, S., Behrens, T., … Smith, S.M., 2009. Bayesian analysis of neuroimaging data in FSL. NeuroImage 45 (1), S173–S186. doi:10.1016/j.neuroimage.2008.10.055.

Woolrich, M.W., Ripley, B.D., Brady, M., Smith, S.M., 2001. Temporal autocorrelation in univariate linear modeling of FMRI data. NeuroImage 14 (6), 1370–1386. doi:10.1006/nimg.2001.0931.

Worsley, K.J., Jezzard, P., Matthews, P.M., Smith, S.M., 2001. Statistical analysis of activation images. In: Functional MRI: An Introduction to Methods. Oxford University Press, pp. 251–270.

Yang, M., Tsai, S.J., Li, C.S.R., 2020. Concurrent amygdalar and ventromedial prefrontal cortical responses during emotion processing: a meta-analysis of the effects of valence of emotion and passive exposure versus active regulation. Brain Struct. Funct. 225 (1), 345–363. doi:10.1007/s00429-019-02007-3.

Zhang, Y., Brady, M., Smith, S., 2001. Segmentation of brain MR images through a hidden Markov random field model and the expectation-maximization algorithm. IEEE Trans. Med. Imaging 20 (1), 45–57. doi:10.1109/42.906424.

Zhao, J., Mo, L., Bi, R., He, Z., Chen, Y., Xu, F., … Zhang, D., 2021. The VLPFC versus the DLPFC in downregulating social pain using reappraisal and distraction strategies. J. Neurosci. 41 (6), 1331–1339. doi:10.1523/JNEUROSCI.1906-20.2020.